Motor Cortical Information Processing*

Jennie Si[1], Daryl R. Kipke[2], Siming Lin[1], Andrew B. Schwartz[3], Peter D. Perepelkin[2]

[1]Department of Electrical Engineering
[2]Bioengineering Program
Arizona State University
Tempe, AZ 85287

[3]The Neurosciences Institute
10640 John Jay Hopkins Drive
San Diego, CA 92121

Abstract

This study examines the neuronal activities of motor cortical cells associated with the production of arm trajectories during drawing movement. Rhesus monkeys were trained to perform different tasks. The electrical signs of discharge of motor cortical cells were recorded while monkeys made movements. We consider a computational model that exacts arm movement trajectories based on recorded neuronal discharge rates. A Self-Organizing Feature Map (SOFM) is used to select the optimal set of weights in the model to determine the contribution of individual neurons to an overall movement representation. The correspondence between movement directions and discharge patterns of the motor cortical neurons is established in the output map. The topology preserving property of the SOFM is used to analyze real recorded data of a behaving monkey performing reaching and drawing movements. In this chapter, we demonstrate the applicability of the SOFM model in analysis of discharge patterns recorded serially by single electrodes. The same principle is then employed in predicting movement trajectories based on 32 channel simultaneous recordings. The procedure of obtaining the 32 or 64 channel chronic recording from each of the hemispheres of rhesus monkeys through microwire electrode arrays is also introduced.

* Research supported in part by the Whitaker Foundation, and by NIH under NINDS-NO1-NS-6-2347. The first and the third authors research is also supported in part by NSF under grant ECS-9553202, EPRI under contract RP8015-03, and a donation from Motorola; the second author by NSF under grant BES-9624636 and NIH R29 DC03070-01.

I. Introduction

Understanding the neural control of movement is one of the outstanding challenges in neuroscience. Seemingly mundane movements such as lifting your arm to scratch the tip of your nose with a finger represents a complex control problem that involves sensorimotor integration, multiple neural pathways, and coactivation of large and small muscles. While this complex problem remains largely unsolved, some important insights can be gained through considering how neural control signals are represented in the responses of neurons in the motor cortex. This chapter focuses on motor cortical signals related to well-defined, two- or three-dimensional arm movements.

Over the last decade or so, several investigators have shown conclusively that motor cortical activity applied to the population vector algorithm (PVA) can be used to generate accurate arm trajectories in point-to-point and drawing movements in both two- and three-dimensional space. The PVA is based on the initial finding by Georgopoulus and colleagues [1] that the direction of the hand during multi-joint arm movements is represented by a simple monotonic relation with the discharge rate of motor cortical cells. This "tuning" function is broad and spans all movement directions, suggesting that many cells represent a given direction simultaneously. The primary descriptor of this function is the movement direction in which a cell fires at its maximal rate—the "preferred" direction. The nature of the tuning suggests that a population of motor cortical cells is capable of encoding uniquely and accurately the movement direction of the hand. This hypothesis has been proven for two- and three-dimensional movements [6, 9, 35]. For each cell, a unit vector in that cell's preferred direction is multiplied by its average discharge rate during the movement. This weighting is done on all the vectors pointing in the preferred directions of the different cells to be included in the population. The weighted vectors are summed and the resulting "population vector" points accurately in the preferred directions. The data for these vectors are generated by recording different cells in individual experiments as animals identically performed the same task repeatedly.

Initially, this algorithm was applied to point-to-point movements and the discharge rate was averaged over the entire movement, a valid simplification since the directions were straight. Recently, there has been a large body of work [36, 27, 31] showing that the trajectory of the hand as it moves during a behavioral task follows rules suggesting that the hand path is the overriding feature of movement controlled by the CNS. We showed originally that a time series of population vectors added tip-to-tail accurately represents 3D point-to-point movements [6]. Schwartz developed a set of drawing tasks and modified the PVA to determine how motor cortical activity is related in an ongoing fashion to the evolution of a movement as it takes place [37, 7]. These findings show that the trajectory of the hand is well represented in the cortical activity and that the shape of the drawn figure is represented in this activity. Furthermore, several of the behavioral invariants characteristic of adult human movements, such as the 2/3 power law [20] and segmentation [30], are also incorporated in this neural signal as well.

These results combine to suggest that relatively simple neural representations in relatively small populations of motor cortical cells can predict realistic arm trajectories during complex reaching and drawing tasks. One of the objectives of our research is to extend this basic finding to

develop a technique to monitor cerebral cortical activity and use it as a control signal for a prosthetic arm. This method would ultimately serve as a long-term amelioration for individuals that are missing or unable to control their arms. Our aim is to refine this control signal so that as funcationally impaired individuals could effortlessly use these prosthetic devices in the same way as functionally intact individuals with near-natural performance.

Neural control of an artificial arm first requires a real-time neural interface to provide simultaneously recorded neural populations, rather than the sequentially recorded populations that have been used in previous studies. With this in mind, we have developed a method of surgically implanting microelectrode arrays in motor cortex to provide chronic recordings of spike-discharge activity from many cortical locations. Second, the desired control information must be extracted from the multichannel cortical recordings. This process must be performed as fast as possible using a minimum amount of information (i.e., from as few cells as possible), and therefore requires the development of intelligent signal processing algorithms. While the PVA approach provides an effective starting point, we are also working to develop analytical techniques to enhance and expand the usefulness of the PVA. One of these is to use an artificial neural network, or more specifically, a self-organizing feature map (SOFM), to efficiently extract the trajectory signal, demonstrated by the PVA, from cortical activity. The self-organizing map of modeled neural activity is based on actual neuronal discharge rates. Self-organizing feature mapping can be used to select the optimal set of weights in the model to determine the contribution of individual elements to the overall movement. The correspondence between the movement directions and the discharge patterns of the motor cortical neurons is then established in the output map.

The remainder of this chapter describes our investigations into motor cortical information processing using simultaneously-recorded neural populations and self-organizing feature maps. Section II briefly describes the experimental procedures for obtaining the neural populations. Section III provides a brief review of some computation models for trajectory prediction from discharge rates, with an emphasis on a self-organizing feature map model. Sections IV and V present two case studies to demonstrate the utility of this model for predicting arm trajectories in two- and three-dimensional arm movements. Finally, Section VI provides some closing remarks.

II. Experimental Procedures

The experimental aspect of our investigations involves obtaining a coarse sample of motor cortical spike-discharge activity as the trained animal performs a 2D or 3D reaching task (Figure 1). A microelectrode array—typically consisting of 16 or 32 microwires—is permanently implanted in motor cortex in order to record isolated single-unit activity at multiple cortical locations. Unit activity is typically observed on 30-75% of the electrodes and it is possible to isolate more than one unit on a single active electrode. The cortical responses are obtained using

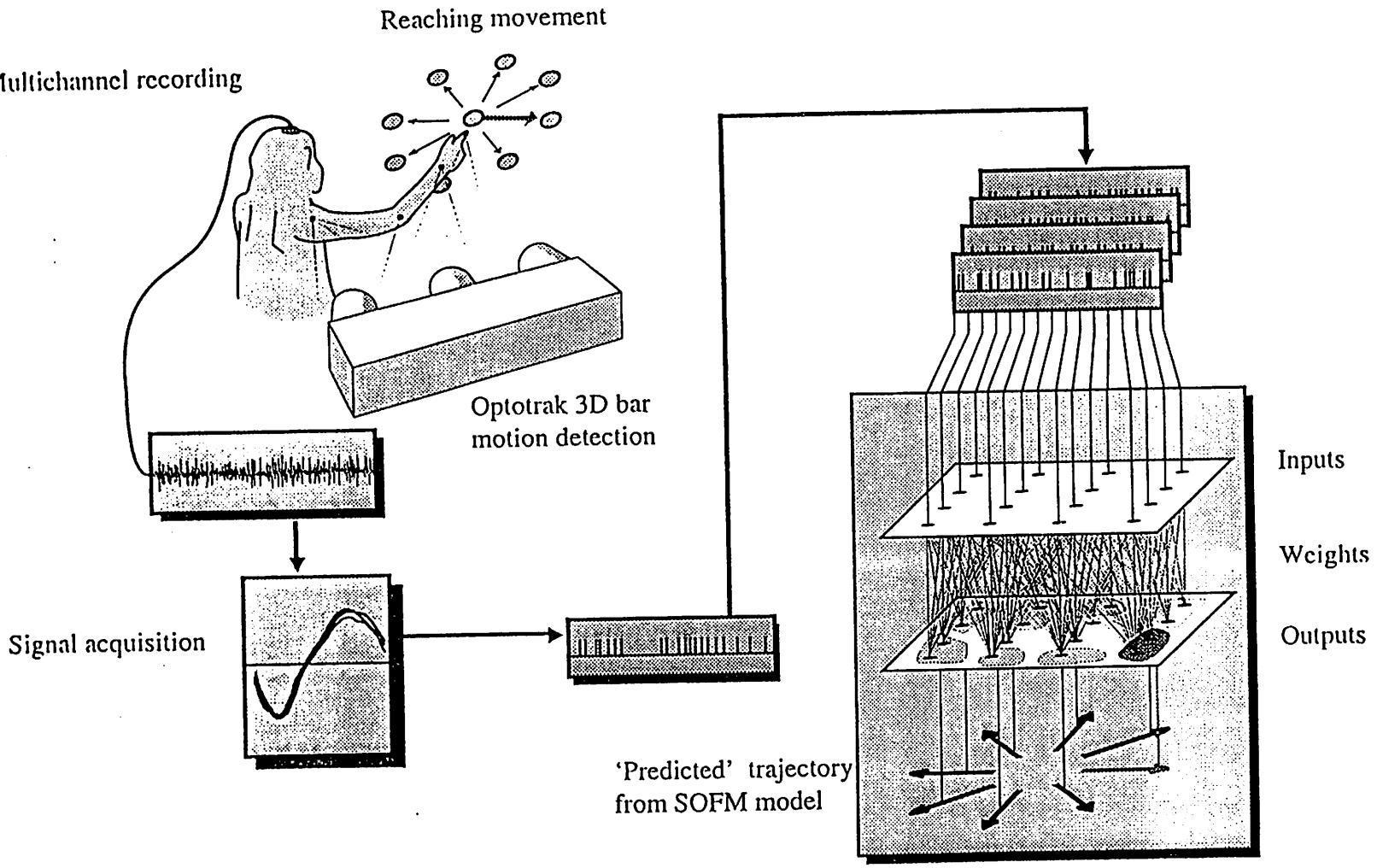

Figure 1. Schematic of an experimental set up to perform real time multichannel neural recording and real time discharge pattern analysis for determining a 'predicted' arm movement trajectory

a special-purpose multichannel neural recording system that provides real-time spike waveform discrimination and streaming of the separate spiketrains to hard disk. Presently, all spiketrain analysis is performed offline. Recordings are obtained daily while the awake animal performs a 3D reaching task.

Figure 2 illustrates sets of spike waveforms that were recorded in the same animal on two different days using a 32-channel electrode. In this case, four channels exhibited spike activity on the earlier day (channels 7, 15, 16, and 29 in left panel), while the same and additional channels were active on a later day (right panel). Figure 3 provides a more detailed view of one of these channels on two different days to illustrate both a well-isolated single unit and multiunit cluster recorded on the same electrode. Unit waveforms on any particular electrode exhibit varying degrees of stability from day to day, with the large unit in Figure 3 being an example of a relatively stable unit.

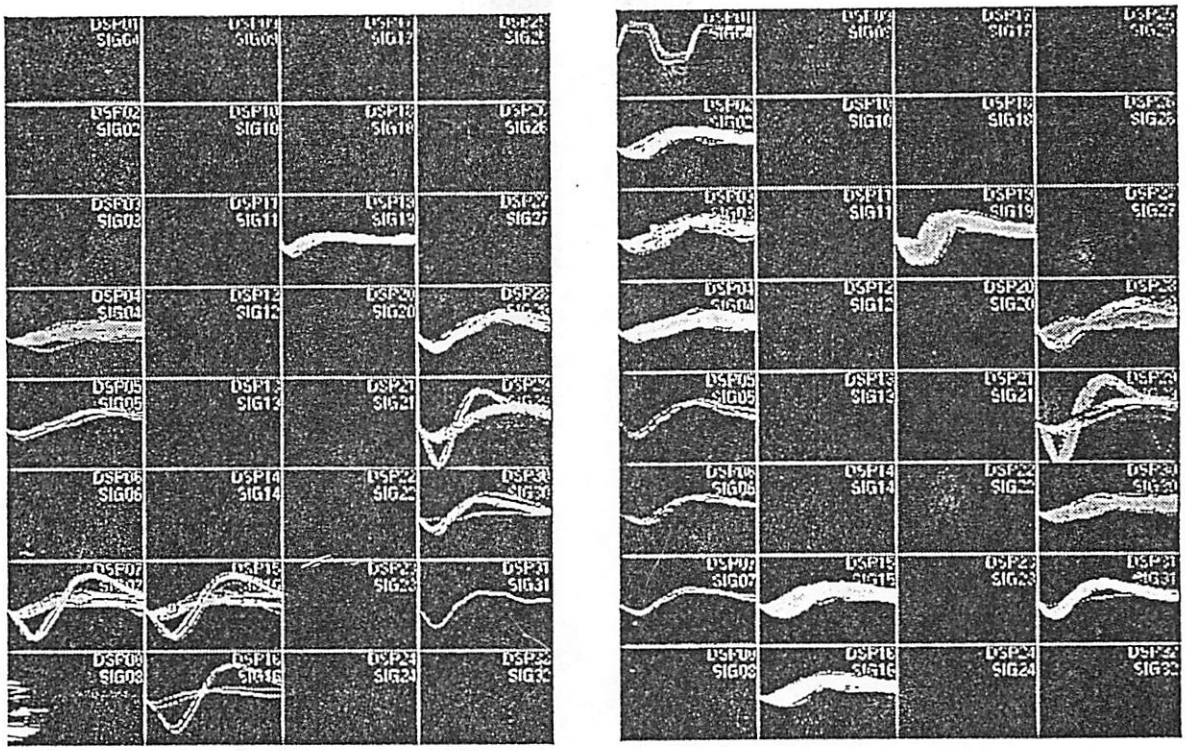

Figure 2. Spike waveforms recorded with a 32 channel electrode on two different days. Each small window represents the spike waveforms recorded from one of the electrodes (voltage vs. time). The length of each window is 0.8 ms.

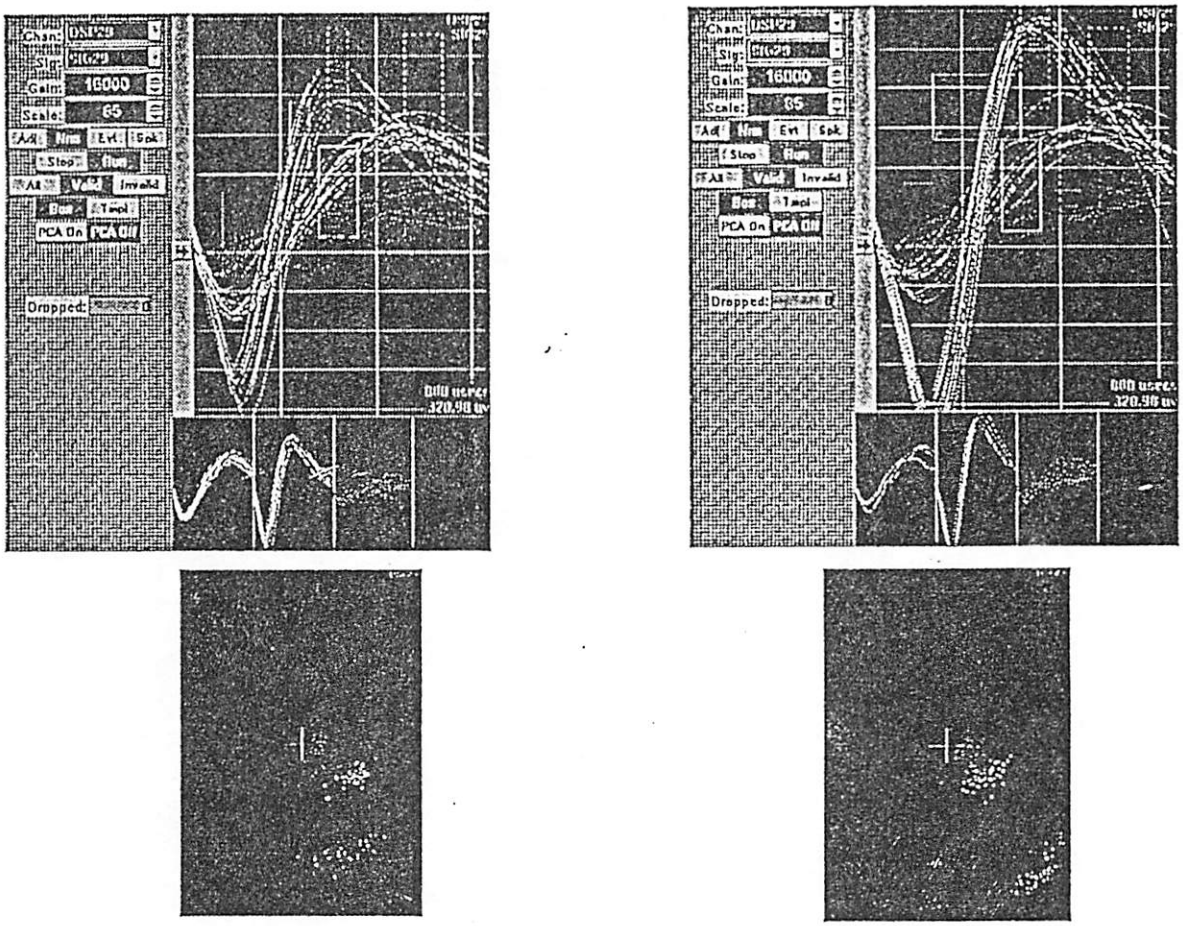

Figure 3. Spike waveforms from one channel recorded on two different days. The top figures are spike waveforms (voltage vs. time) obtained using a simple negative threshold. These raw waveforms are further discriminated in real-time on the basis of waveform features. The bottom figures are projections of the first two principal components the waveforms. The discrete clusters away from the origin represent different waveforms.

The arm reaching task was carried out by monkeys well-trained in the task. A 3D center→out task was prescribed whereby the monkey was trained to move its forelimbs in one of eight different movement directions. Five acrylic posts with lighted marker buttons at the ends were mounted to a disk which was free to rotate +/- 90 degrees from a neutral position. Two posts were long, two posts were short, and one central post had a length midway between the other two. When the disk was stopped in the +90 degree position, the marker buttons were positioned at four of the corners of a five inch cube circumscribed about the central marker. When rotated to the -90 degree position (180 degrees from the +90 degree position), the four outer markers were positioned at the other four corners of the five inch cube (Figure 4).

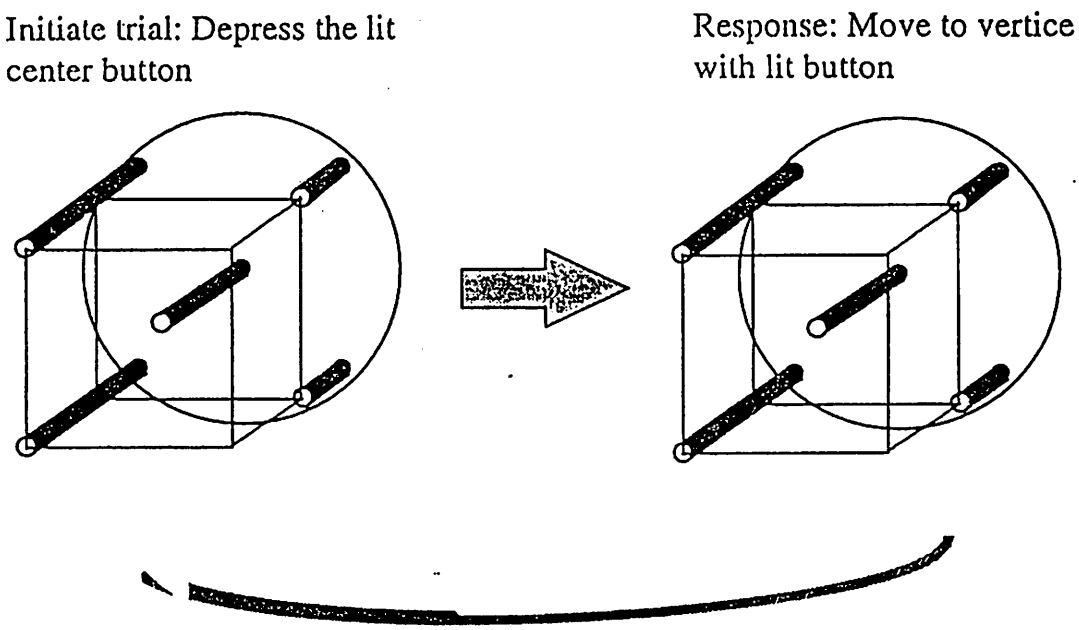

Figure 4. Pushbutton switches with lights are mounted at the ends of five plexiglass cylinders. Four switches are located a the vertices of a cube five inches on a side, and one switch is located on the central rod.

In the 3D center→out task, the disk was first rotated to the proper position remotely, and the central button was lit. When the monkey placed its finger on the central marker, the central button turned off and one of the "corner" buttons were lit. The monkey's task was to release its hand from the central marker and move it to press the button that was lit within a time-out interval. Five trials in random order were recorded for each of the eight movement directions. Recordings of the movement times and the cortical cell activity from both hemispheres were recorded simultaneously.

III. Computing Arm Trajectory from Neural Discharge Rates

The trajectory of the arm is an important element in the control of volitional reaching and pointing and is thought to be controlled continuously during the movement. The arm trajectory may be decomposed temporally into a series of vectors. Each vector is specified by a direction and a magnitude; these components define tangential velocity. If the vectors are defined at constant temporal intervals, the magnitude of each vector is speed. Although it is useful to study speed and direction separately, in certain movements such as drawing they may not be independent. As the spatial rate of directional change (curvature) increases, the angular velocity decreases [33,34]. As will be shown in the following, both movement direction and movement speed are represented in the output map of the SOFM, once the network is trained, as it is continuously represented in the activity of motor cortical neurons during the tracing movement.

3.1. Population Vector Analysis

The population vector method was developed by Georgopoulos and his collaborators to investigate the relations between the neuronal activity in the motor cortex of the monkey and the direction of arm movements in two- and three-dimensional spaces [1-9].

In the study of reaching movement in a two-dimensional space, monkeys were trained to make point-to-point movements from a center start position to one of eight targets spaced equally around a circle. Neurons recorded during this task were found to have mean discharge rates that were highest in a single 'preferred' direction and tapered off gradually in directions farther away from the preferred direction, firing at their lowest rates for the movement directions 180° from the preferred direction. The relation between movement directions and discharge rates for individual neurons could be fit with a cosine tuning function:

$$D = b_0 + k\cos(\theta - \theta_0)$$

where b_0 is a regression coefficient corresponding to the mean activity in the task, k is a regression coefficient corresponding to the depth of the modulation across different movement directions, θ is the direction of the movement, θ_0 is the preferred direction and D is the discharge rate.

The tuning function of individual motor cortical neurons spans the entire directional domain. Each directional neuron encodes all directions of the movement. Conversely, all neurons in the cortical population simultaneously encode a single movement. If C_i is the unit preferred direction vector for the i-th neuron, then the neuronal population vector $P(t)$ is determined as the weighted sum of these vectors:

$$P(t) = \sum_i r_i(t) C_i$$

where the weight $r_i(t)$ is the activity (discharge rate minus the geometric mean) of the i-th neuron at time bin t. The discharge rate can be measured during monkey's arm movements, resulting in a series of weighted vectors for each neuron. When these vectors are summed across the population for each bin, the resulting series of population vectors $P(t)$, represent well the direction of the movement as it changes in time during the task. Moreover, the magnitudes of these population vectors suggest instantaneous displacement (speed) throughout the task. Thus, connecting these population vectors tip-to-tail together, one may obtain a predicted neural trajectory. It was shown that real trajectories of arm movement could be predicted by neural trajectories.

To use the population vector approach described above, one needs to know the preferred direction of every neuron in the selected cortical population. Usually this is done by experiments. Any bias resulting in a non-uniform distribution of preferred directions could result in prediction error in the trajectory.

There have been some other methods used for population decoding. For example, the simulated annealing algorithm has been used to adjust the connection strengths of a feedback neural

network so that it would generate a given trajectory by a sequence of population vectors [22]. However, as in the population vector algorithm, the preferred direction is required in this algorithm.

3.2. The Optimal Linear Estimator (OLE) Method

The OLE is a statistical method for population decoding [23]. The estimation formula of OLE is as follows:

$$V_{est} = \sum_i r_i(t) D_i$$

where V_{est} is the estimate of the movement direction, r_i is the measured firing rate (or normalized firing rate) of neuron i. Note that D_i is different from the preferred direction. Specifically,

$$D_i = \sum_j Q_{ij}^{-1} L_j$$

with

$$L_j = \int V f_j(V) dV$$

and Q is the correlation matrix of firing rates determined as

$$Q_{ij} = \int r_i r_j P(r|V) dr dV$$

where V denotes the actual movement direction, $P(r|V)$ denotes the probability of obtaining the firing response r given that the movement direction takes the value V, and $f_i(V)$ is the average discharge rate of cell i when the movement direction takes the value V. Equivalently,

$$f_i(V) = \int r_i P(r|V) dr .$$

It is shown that the cosine tuning curve is the optimal case for linear decoding methods and the OLE method can produce the smallest average error of any linear method [23]. However the OLE method may encounter difficulty when the number of cells used is large and when Q is ill-conditioned. When the unit spiketrains are noisy (missing spikes, false-positive spikes), the recorded discharge rates may not be perfect cosine tuning curves and the assumption made for guaranteeing the performance of OLE is no longer true.

3.3. The Self-Organizing Feature Map (SOFM) Model

The SOFM has been applied successfully to speech processing [11], robotics [19], vector quantization [17, 21] and biological modeling [18]. The SOFM learns a mapping from the input data space R^n onto a two-dimensional array of nodes by means of self-organization which is driven by examples $X \in R^n$ (Figure 5). In SOFM, every output node p is associated with a synaptic weight vector $W_p = [w_{p1}, w_{p2}, ..., w_{p3}]^T \in R^n$. The learning rule or the weight adaptation for SOFM in the discrete form is given by [12-15]:

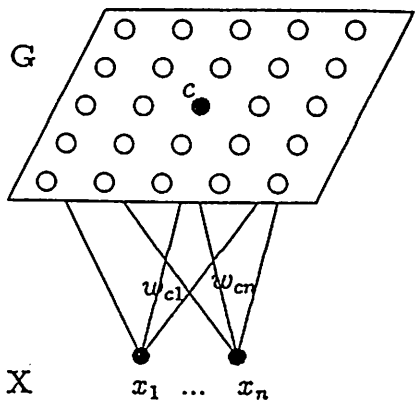

Figure 5. Self-Organizing Feature Map

$$w_p(t+1) = w_p(t) + \alpha(t)[X(t) - w_p(t)], \qquad \forall p \in N_c(t)$$
$$w_p(t+1) = w_p(t), \qquad \forall p \notin N_c(t)$$

where t=0,1,2,... is the discrete time coordinate, $\alpha(t)$ is the learning rate factor, and $N_c(t)$ defines a set of neighborhood nodes of the winner node c. The winner node c is defined to be the node whose weight vector has the smallest Euclidean distance from the input $X(t)$:

$$\|w_c(t) - X(t)\| < \|w_p(t) - X(t)\| \qquad \forall p .$$

We have used a 20 by 20 two-dimensional lattice as the output layer and $\alpha(t) = 0.95(1 - t/N)$ with N=200000 in obtaining our results in sections 4 and 5 [16]. We started with the initial radius of $N_c(t)$ that equals the diameter of the output layer and let it shrink with time.

In our applications, the SOFM acts as a decoder. By finding the winners, SOFM maps the input onto a node in the output layer. Every node in the output layer decodes an association with inputs. The critical feature of this algorithm is the topology preserving. We call a map topology preserving if: a) similar input vectors are mapped onto identical or neighboring output nodes; b) neighboring nodes have similar weight vectors. Property (a) ensures that small changes in the input vector causes correspondingly small changes in the location of the output winner. This makes SOFM robust against distortions of inputs. Property (b) ensures robustness of the inverse mapping which is critical for the accuracy of SOFM as a decoder. The SOFM model approach extracts directional patterns that are encoded in the discharge rates with the following advantages: 1) without using the preferred directions; 2) robust against noise; 3) easy to implement in hardware. The population vector method suggests that there is a close association between the discharge rates of cells in motor cortex and the direction of arm movement.

IV. A Preliminary Case Study Using SOFM for Single Channel Recordings

We consider a self-organizing model of the neuronal discharge patterns based on neuronal discharge rates. The inputs to the model are averaged discharge rates from a group of cells in the monkey's motor cortex. These discharge rates were taken while the animal was performing a behavioral task. The output map of the model is either a two-dimensional plane or a three-dimensional cube. The map codes not only the predicted direction of arm movement, but also other non-specific movement associated parameters such as speed and position. The nodes in the output map are interconnected by a neighborhood function during training. SOFM was used to adapt the weights of the network to generate a mapping between discharge rates of motor cortical neurons and directions of arm movement.

The main advantage of this approach is that preferred directions are not prerequisites for obtaining predicted directions. Consequently the possibility of error accumulation from non-uniformities in preferred directions is reduced. Moreover, the topology preserving property of the SOFM enables us to calibrate the output map with the topology relation within input discharge rates, which is useful when interpreting the computation results.

In this study we focus on the statistical discrimination of behavioral modes while the monkey performs behavioral tasks as described in the corresponding sections. Our computer simulations from a former spiral task reveal that the behavioral modes are clearly differentiated and the map simultaneously provides a clear topological relationship among these modes. The movement directions during the spiral tracing task is well predicted by the discharge rate patterns using the self-organizing model (refer to section 4). The population vector method has already been used to show that directions and speed are well represented in the activity of these cells [7]. This method assumes the linear functional relationship between discharge rates and movement directions as shown in the equation to obtain $P(t)$. It may not capture all the consistent relationships between cell activity and different parameters that could be represented in this activity. In contrast, the statistical nature of the SOFM technique will capture these relationships without *a priori* assumptions about what is represented or the form of the code.

A rhesus monkey was trained to trace with its index finger on a touch-sensitive computer monitor. In the spiral tracing task, the monkey was trained to make a natural, smooth drawing movement within approximately a 1-cm band around the presented figure. As the figure appeared, the target circle of about 1-cm radius moved a small increment along the spiral figure, and the monkey moved its finger along the screen surface to the target. The spirals we studied are outside→in spirals.

Due to limitations in single electrode recording, the firing activities of the recorded n cells could not be taken simultaneously. Consequently the average discharge rate vector X_j could not be calculated simultaneously at time t_j. However, special care was given to ensure that the monkey repeated the same experiment n times to obtain the firing signal for all the n cells under almost the same experimental condition. We thus assume that the experiments of recording every single cell's spike signal were identically independent events so that we could use spike signals of the n cells as if they were recorded simultaneously.

While the well-trained monkey was performing the previously learned routine, the occurrence of each spike signal in an isolated cell in the motor cortex was recorded. The result of these recordings is a spike train at the following typical time instances, $\tau_1, \tau_2, \cdots, \tau_L$. The average discharge rate is calculated from the raw spike train for every time interval (selected as 20 msec in our simulations).

Let Ω be the collection of the monkey's motor cortex cells whose activities contribute to the monkey's arm movement. Realistically we can only record a set of sample cells $S = \{S_i \in \Omega, i = 1,2,\cdots,n\}$, to analyze the relation between discharge rate patterns and the monkey's arm movements. We assume that the cells included in the set S constitute a good representation of the entire population. Our following results are obtained from 81 cells in the motor cortex. Each complete trial of movement in the tasks take about 200 msec. Discharge rate vectors are the inputs to the SOFM and the outputs from the SOFM are predicted moving directions corresponding to the discharge rate pattern.

4.1. SOFM for Neuron Discharge Rate Pattern Analysis

The objective here is to investigate the relationship between monkey's arm movements and firing patterns in the motor cortex . The topology preserving property of the SOFM is used to analyze real recorded data of a behaving monkey [16].

To train the network, we select n cells (in this case study, n=81) in the motor cortex. The average discharge rates of these n cells constitute a discharge rate vector $X_j = [d_{1j}, d_{2j}, \cdots, d_{nj}]^T$, where d_{ij}, $i=1,...,n$, is the average discharge rate of the i-th cell at time bin t_j. A set of vectors $\{X_k | k = 1,2,\cdots, NP\}$ recorded from experiments are the training patterns of the network, where NP is the number of training vectors. In this case study, a 20 by 20 two-dimensional lattice was used as the output layer of the SOFM.

During training, a vector $X \in \{X_k | k = 1,2,\cdots, NP\}$ is selected from the data set at random. The discharge rate vectors are not labeled or segmented in any way in the training phase: all the features present in the original discharge rate patterns will contribute to the self-organization of the map. Once the training is done, as described previously, the network has learned the classification and topology relations in the input data space. Such a 'learned' network is then calibrated using the discharge rate vectors of which classifications are known. For instance, if a node i in the output layer wins most for discharge rate patterns from a certain movement direction, then the node will be labeled with this direction. In this part of the simulation, we used numbers 1~16 to label the nodes in the output layer of the network, representing the sixteen quantized directions equally distributed around a circle. For instance, a node with label '4' codes the movement direction of 90 degrees from the horizontal position. If a node in the output layer of the network never wins in the training phase, we label the node with number '-1'. In the testing phase, a '-1' node can become a "winner" just as those marked with positive numbers. Then the movement direction is read out from its nearest node with a positive direction number.

Figure 6 gives the learning results using discharge rates recorded from the 81 cells in the motor cortex in one trial of the spiral task. From the output map, we can clearly identify three circle-shaped patterns representing the spiral trajectory. These results show that the monkey's arm movement directions are clearly encoded in firing patterns of the motor cortex. A clear pattern can be distinguished from the locations of the nodes in the map. Note that nodes with the same numbers (i.e., directions) on different spiral cycles are adjacent. This is the same for the actual trajectory and can be considered preservation of topology, which is an attribute of the SOFM. Different cycles of the spiral are located in correspondingly different locations of the feature map, suggesting that parameters in addition to directions influence cortical discharge rates.

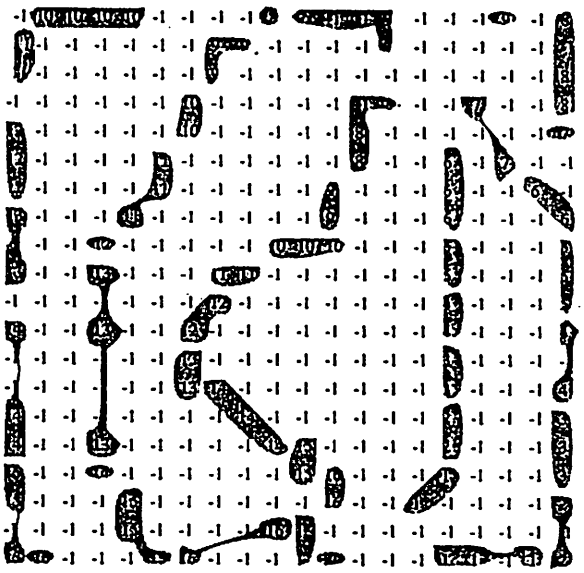

Figure 6. The SOFM output for the discharge rates of the 81 neurons in the motor cortex in the spiral task. The size of the output map is 20 by 20. The nodes marked with positive numbers are cluster 'centers' representing the directions as labeled, while the nodes labeled with '-1' are the 'neighbors' of the 'centers'. The closer it is to the 'center', the more possible it represents the coded direction of the 'center'.

What follows are some analytical results using data recorded from five trials in spiral tracing tasks and center→out tasks.

4.2. Analytical results

Analytical study 1. In this analysis, we used data recorded during five trials of spiral tracing tasks. The first trial was used for testing and the rest were used for training. After the training and labeling procedure, every node in the output map of the SOFM was associated with one specific direction. The direction of a winner was called "neural direction" when discharge rate vectors were presented as the input of the network bin by bin in the testing phase. Figure 7 gives "neural directions" against corresponding monkey's finger movement directions.

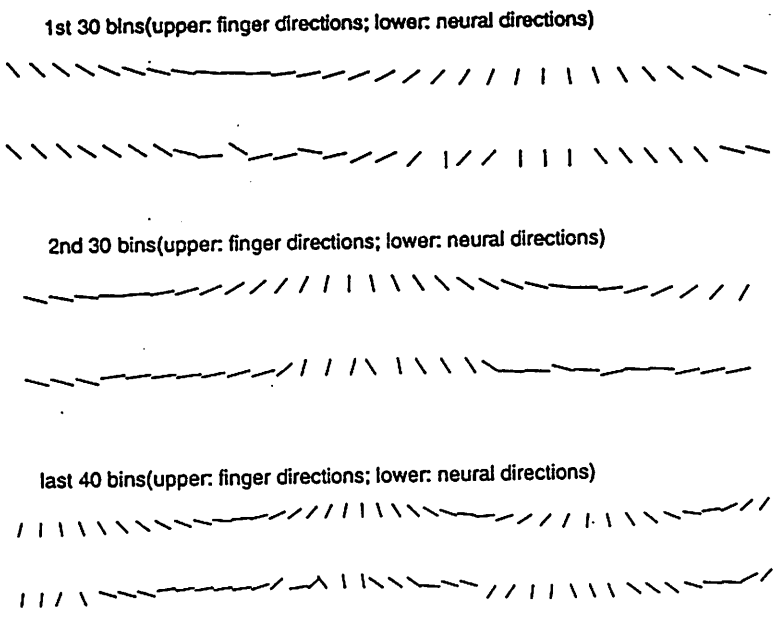

Figure 7. The "neural directions" and the finger directions in 100 bin series in the inward spiral tracing task.

After post-filtering the predicted "neural directions" with a moving average filter with a width of three bins, we combined the neural directions tip-to-tail bin by bin. The resulting trace ("neural trajectory") is similar to the finger trajectory. Note that the "neural directions" are unit vectors. To use vectors as a basis for trajectory construction, the vector magnitude must correspond to movement speed. However, in applying the SOFM in the present analysis, we did not calibrate the speed information, or the speed is approximately considered unity. Figure 8 demonstrates the complete continuous monkey's finger movement and the predicted neural trajectory.

Analytical study 2. In addition to the spiral data used above, the data recorded in the 2D center→out tasks were added to the training data set. Figure 9 shows that the overall performance of the SOFM has been improved. This result suggests that the coding of arm movement direction is consistent across the two different tasks.

Analytical study 3 (leave-k-out method). This analysis used a total of five different sets of experiments for training and testing the SOFM. Each data set consisted of five trials in each of the spiral and center→out tasks. In each simulation, one of the trials in the spiral task was selected for testing and the rest were used for training. Note that the training and testing data were disjoint in each set of experiment. The neural trajectories from the five tests were averaged and Figure 10 shows the averaged result. Due to the nonlinear nature of the SOFM network, a different training data set may result in a different outcome in the map. Therefore, the leave-k-out method provides us with a realistic view on the overall performance of the SOFM. Figure 11 shows the bin-by-bin difference between the neural directions and the finger directions in 100 bins. The dashed line in the figure represents the average error in 100 bins.

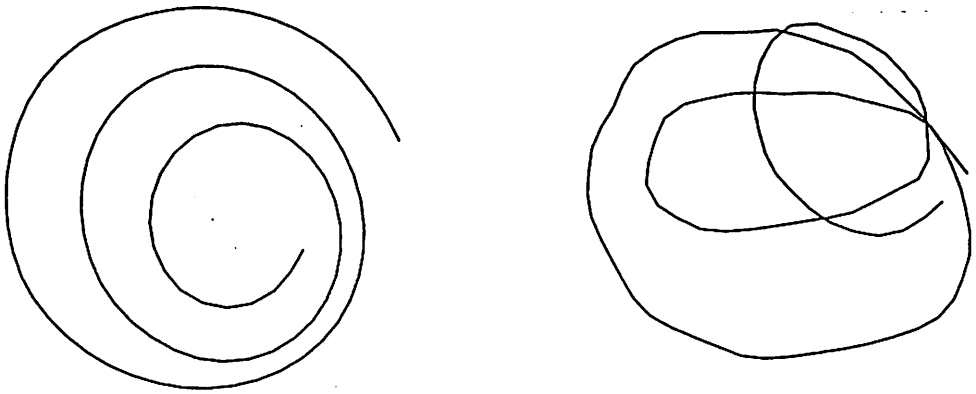

Figure 8. Using data from spiral task for training. Left: the monkey's finger movement trajectory calculated with constant speed; right: the SOFM predicted "neural trajectory".

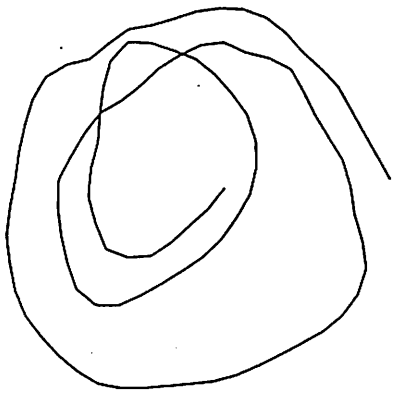

Figure 9. Neural trajectory: using data from spiral and center → out tasks for training.

Note from Figure 6 that when the monkey's finger was moving along the same direction on different cycles of the spiral, one observes distinct cycles on the output map of the SOFM as well. By the topology preserving property of the SOFM, this suggests that the output nodes decode not only directions but also probably speed, curvature and position, etc. Although the population vector method has previously shown this information to be present in motor cortex [7], the SOFM model is able to capture regularities about speed and curvature without assuming any linear functional relationship to discharge rates as the population vector and the OLE methods do.

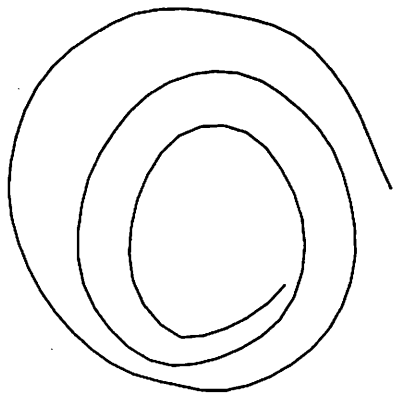

Figure 10. Neural trajectory: average testing result using leave-k-out method.

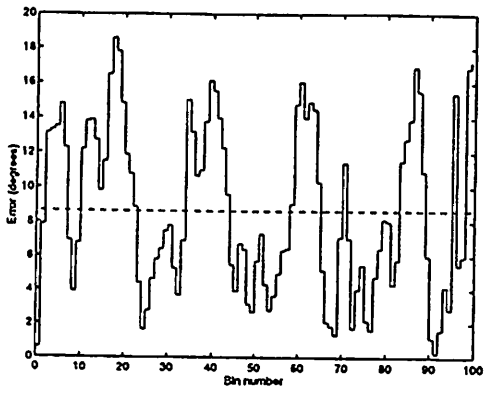

Figure 11. The binwise difference between the finger directions and the neural directions in 100 bins. The dashed line is the average error in 100 bins. The neural trajectory is the average testing result of the SOFM using the leave-k-out method.

For those drawing movements with significant changes in speed, we may be able to quantize the speed as we did with directions. As we have discussed previously, the direction and the curvature or speed may be encoded in discharge rates as a feature unit, allowing the nodes in the output map to be labeled using directions and speed together. Consequently, the same process of direction recognition by using the SOFM could be applied to speed recognition based on discharge rates of the motor cortex.

Other types of networks, e.g., the sigmoid feedforward and radial basis function networks could have been used to associate discharge rates with movement directions. However, as discussed above, the SOFM offers a unique combination of both data association (which some other networks can achieve) and topology information as represented by the two-dimensional output map (which is hard or impossible for other networks to implement).

V. Analysis of Simultaneously Recorded Neural Populations Using SOFM

The previous results were obtained based on single-neuron recordings of 2D spiral and center→out tasks. In the present section we provide some statistical analysis on simultaneous recordings from motor cortex.

5.1. Spike Rasters and Preferred Directions for 3D Reaching Tasks

Simultaneously recorded units in motor cortex exhibit directional tuning as expected. Figures 12 through 14 are spike raster plots to demonstrate the forms of the raw spike activities. In Figure 12, eight separate figures are displayed to show the spike activity as the monkey moved its hand to each of the eight individual targets located at the corners of a cube circumscribed around the central starting position (see Figure 4 for the experimental arrangement). The four central plots represent the four targets on the back side of the cube. Target numbers are located on the upper right-hand corners of each plot. For instance, target #1 is the lower right-hand target on the front face of the cube and is displayed on the lower right corner of the eight-figure raster plot.

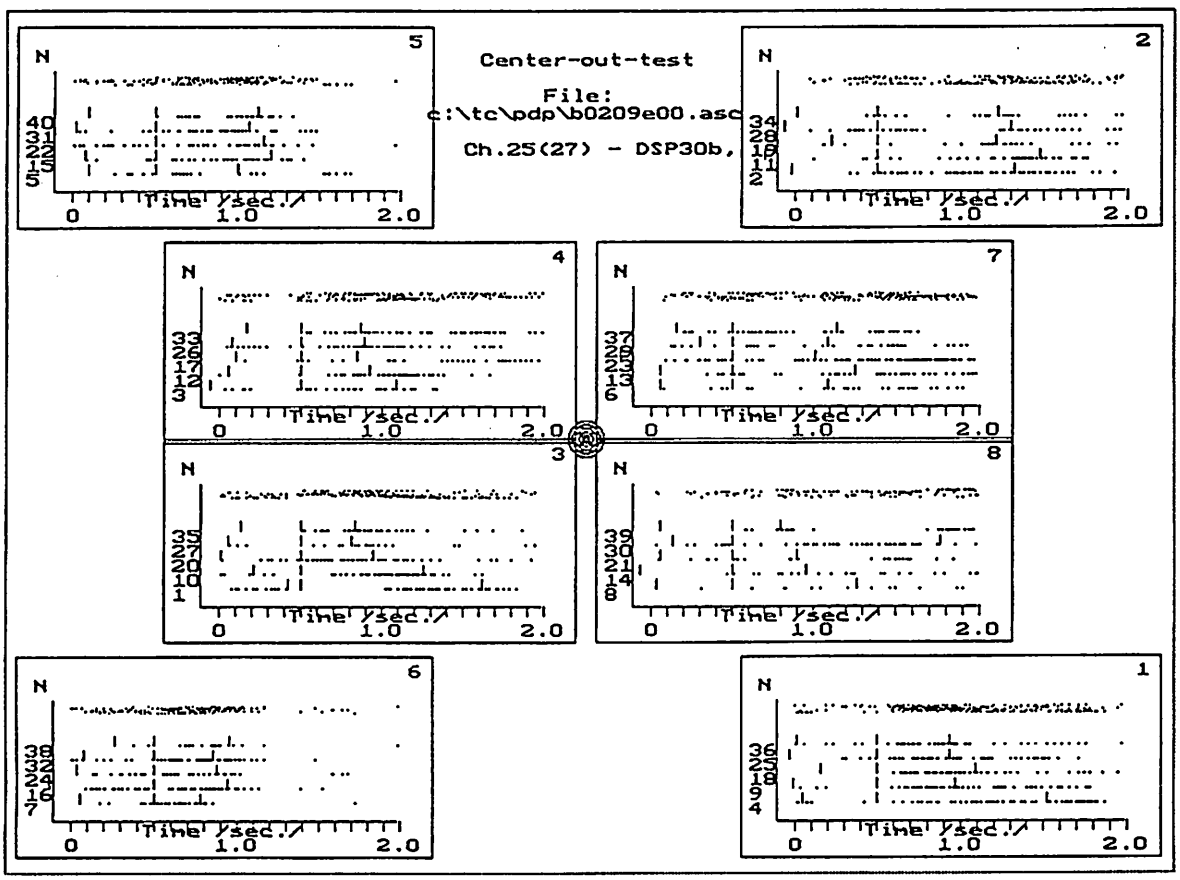

Figure 12. Raster plot of a single-cell's spike activity recorded from the motor cortical area during the 3D reaching task

Five trials were recorded for each target location in random order. The trial numbers are listed on each line as numbers 1 to 40. Each dot on a plot represents a spike that was detected during the movement. Vertical hash marks show events during each trial: First mark - light on target button appears; second mark (the vertical center line about which all trials are synchronized) - monkey released center button and initiated move toward target; third mark - hand arrives at and presses target button. Therefore, the distance between hash marks before the vertical center line is the reaction time, and the distance between marks after vertical center line is the movement time.

The bands above each target's plot shows the spike activity traces redisplayed in a compressed format. These bands clearly show darkly when the frequency of the unit spike activity is high and sparsely when the unit spike activity is low. The maximal activity interval is different for each of the eight targets, which suggests that there is a preferred direction for this cell. The cell activity patterns would be fairly uniform during movements to all eight targets if direction was unrelated to the cell firing rate. We thus would say that this cell is directionally tuned.

Four cells recorded from the motor cortical area of the left and right hemispheres are represented in Figures 13 and 14, respectively. Each speckled horizontal band represents the activity of one cell during five trial movements. The eight boxes contain the firing patterns observed during hand movements to each of eight targets during the 3D reaching task. The layout of these boxes has the same legend as Figure 12. Therefore the top horizontal band in each of the eight plots contains the activity of cell #1, whereas the bottom bands contain the activity of cell #4. Each dot represents a single spike in the record.

Figures 13 and 14 differ from Figure 12 in that two sets of raster plots are provided for each target location. The leftmost series of four bands in each of the eight plots shows the spike activity of the cells when the left arm of the monkey was utilized; the rightmost series of four bands in each plot shows the activity when the monkey used its right arm. The interesting observation from Figures 13a, 13b and Figures 14a, 14b is that the spike activity suggests that the 10 cells recorded and shown in Figures 13 and 14, respectively, are directionally tuned during motions of both the right and left arms.

In a sample neural population of 25 units, the units tended to be directionally tuned and the resulting set of preferred directions provided a coarse sample of the 3D work space (Figure 15).

5.2. Statistical analysis of neuronal activity patterns in 3D reaching using SOFM

The SOFM is effective for estimating arm trajectories from simultaneously recorded neural populations of motor cortical cells. In the 3D reaching tasks, five trials were recorded during movements to each of the eight target locations to yield experimental data sets consisting of 40 successful trials. In all the following results, we have used a 20 by 20 output map for the SOFM network. The inputs to the SOFM range from 12 to 23 simultaneously recorded units. Discharge rates—the inputs to the SOFM network—were computed from the number of spikes from the time the target button was lit to the time the target button was pressed.

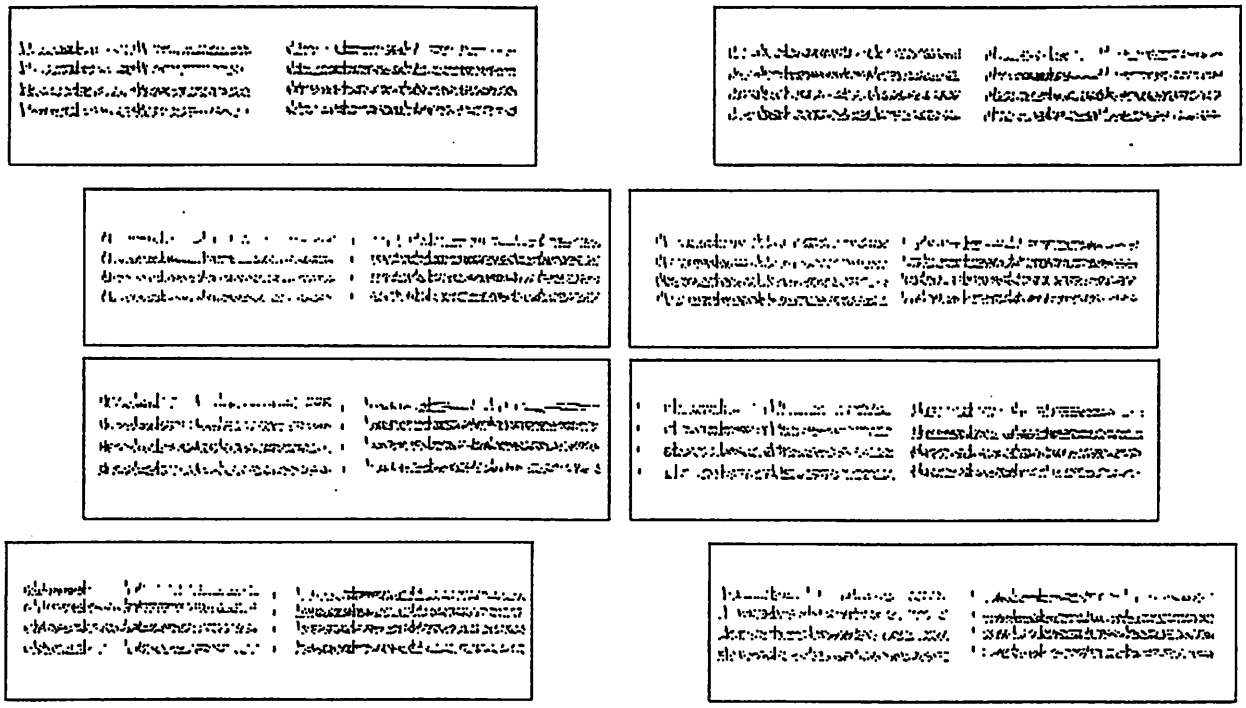

Figure 13a. Raster plot of spike activities of four cells from the left hemisphere during 3D reaching motions of the left and right arms.

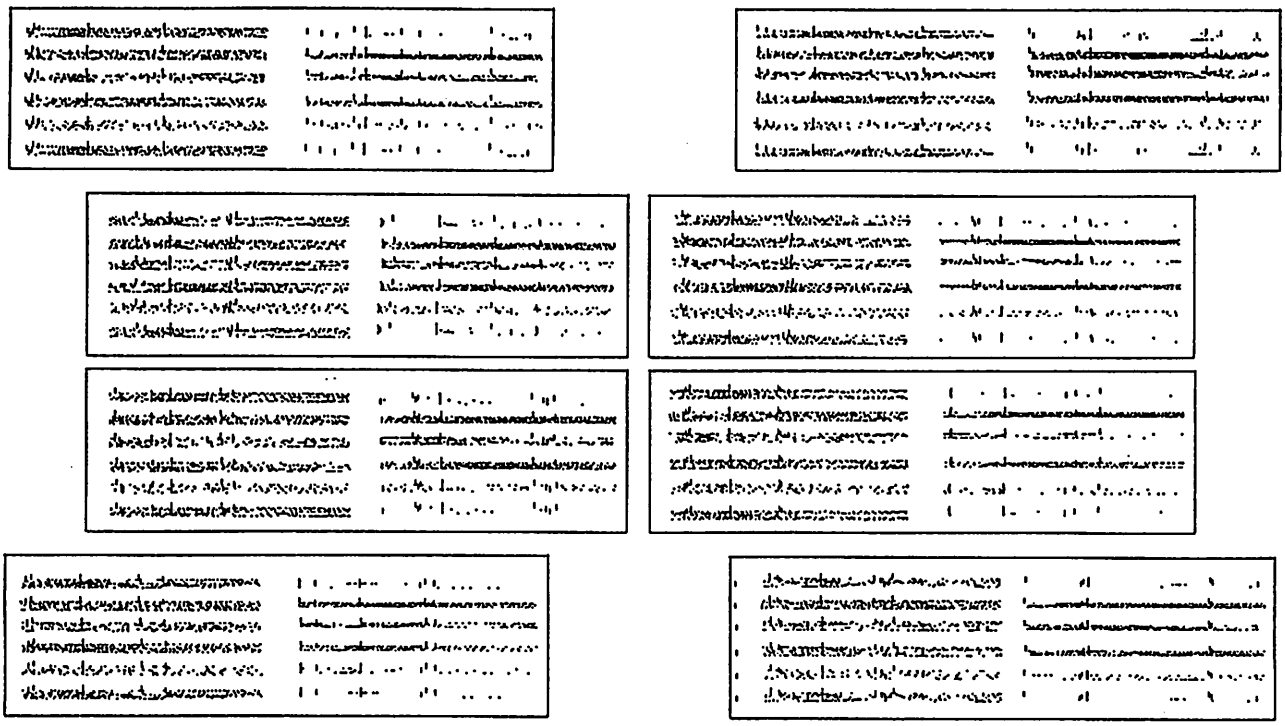

Figure 13b. Continuation of Figure 13a with additional six cells.

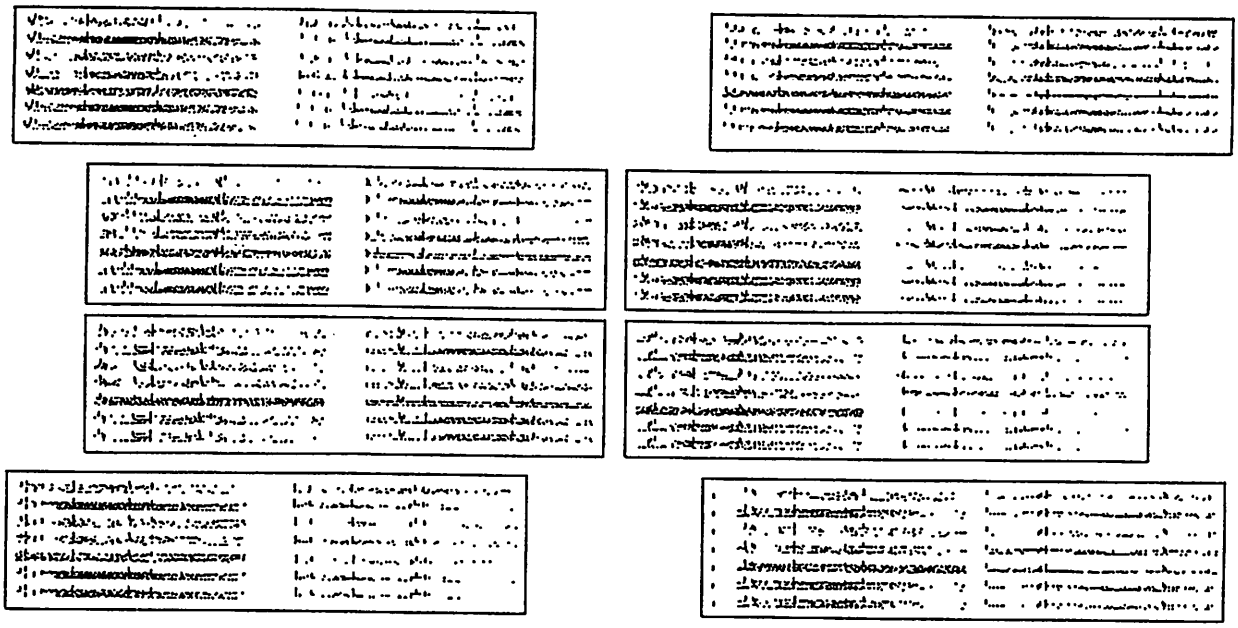

Figure 14a. Raster plot of spike activities of four cells from the right hemisphere during 3D reaching motions of the left and right arms.

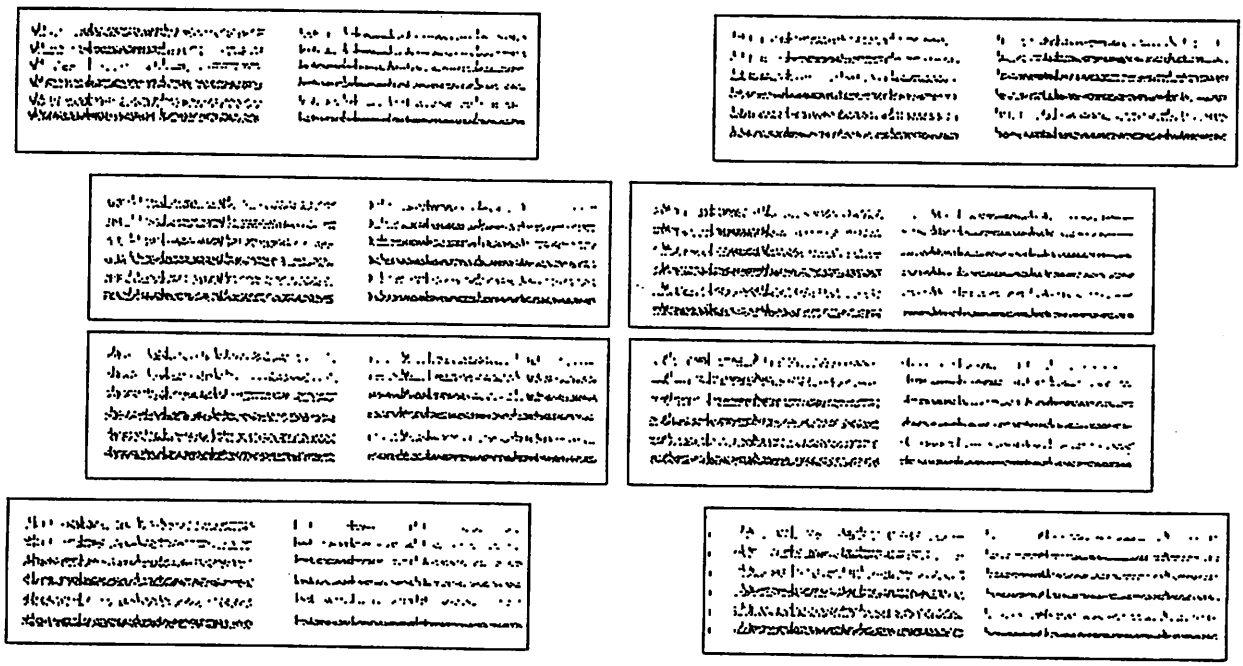

Figure 14b. Continuation of Figure 14a with additional six cells.

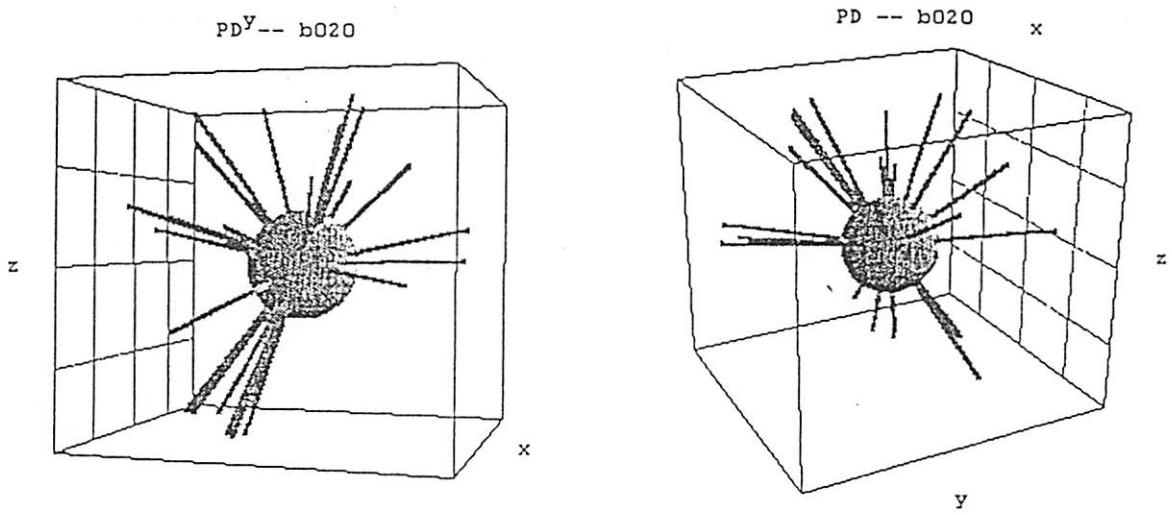

Figure 15. Two different views of the set of preferred directions for a simultaneously recorded neural population recorded in motor cortex. The preferred directions are plotted in the 3D workspace with the center of the cube corresponding to the center target. The hatched face of the cube corresponds to the back plane of the workspace.

Analytical study 1 (one experiment for training, one experiment for testing). These simulations use one experimental data set for training the SOFM and a second independent experimental data set for testing. Individual as well as averaged testing results as included in Table 1. where in Table 1, "exact-on-target" is the number of testing trials which are correctly predicted by the trained SOFM; "1st-neighbor-target" records the number of testing trials which are one direct neighbor distance away from the real reaching direction; "2nd-neighbor-target" are those which are identified as the diagonal element of the real reaching direction; the "input #" represents the number of active units or the number of inputs to the SOFM network.

Analytical study 2 (three experiments for training, one experiment for testing). These simulations used three experimental data sets for training the SOFM and a fourth independent experimental data set for testing. Individual as well as averaged testing results as included in Table 2. In these simulations, 62% of the testing trials are correctly predicted by the SOFM, over 90% of the testing trials have been correctly predicted within the distance of 1st neighbor. The results obtained here are consistent with the ones obtained in Section IV which involved only single channel recordings.

These two simulations were conducted without any pre- or post-processing of the neural data. As can been seen from Tables 1 and 2, when more training data are available for the network, the prediction accuracy of the SOFM significantly improves (62% vs. 42% for exact-on-target hits).

for the reaching movements. The SOFM may be used as an very efficient tool to provide a correlation between the movement direction and the neuronal activity patterns.

Table 1. Testing result summary using one experiment for training after the SOFM trained by one different reaching experiment.

	Exact on	1st neighbor	2nd neighbor	Total #	
Training/testing file names	target	target	target	target	input #
b0202e00 / b0202e01	21	7	11	39	14
b0117r01 / b0117r02	16	18	5	39	12
b0117r03 / b0117r04	28	9	2	39	12
b0129e02 / b0129e00	18	10	6	34	16
b0205e00 / b0205e01	8	17	14	39	15
b0130e00 / b0130e01	15	8	3	26	18
b0119r03 / b0119r00	4	9	16	29	23
b0118r02 / b0118r01	0	16	23	39	17
b0131e01 / b0131e00	17	10	3	30	19
b0201e00 / b0201e01	24	9	6	39	15
Total	151	113	89	353	
Accumulative percentage	43%	32%	25%		

Table 2. Testing results summary using 3 experiments for training and an independent reaching experiment for testing

	Exact on	1st neighbor	2nd neighbor	Total #	
Training/testing file names	traget	target	target	of trials	input #
b0118r00+01+02 / 03	8	2	2	12	17
b0129e00+01+02 / 03	12	10	2	24	16
b0118r01+02+03 / 00	27	7	5	39	17
b0118r00+02+03 / 01	26	10	3	39	17
b0118r00+01+03 / 02	27	12	0	39	17
b0129e01+02+03 / 00	20	12	2	34	16
b0129e00+02+03 / 01	11	11	2	24	16
Total	131	64	16	211	
Accumulative percentage	62%	30%	8%		

VI. Concluding Remarks

Our results based on raw spike data recorded from rhesus monkey's motor cortices have revealed that the monkey's arm trajectory is encoded in the averaged discharge rates. Hebb hypothesized

in 1949 that the basic information processing unit in the cortex is a cell assembly which may include thousands of cells in a highly interconnected network [24]. This cell-assembly hypothesis shifts the focus from a single cell to the complete network activity. In our studies, information from 81 cells or around 16 cells (corresponding to single or multichannel recording, respectively) in the monkey's motor cortex has been used to predict its arm movement directions using a SOFM model. Our results show that a limited number of neuronal cells have characterized the monkey's motor cortical activities quite well in a spiral arm movement and in 3D reaching movement. Other studies using different neural ensemble analyses, such as synfire chain [10] and multi-cell correlation [25], have also revealed the significance of the amount of information provided by local measurements with a limited number of cells in the associative cortex. It is quite intriguing that a small set of cells could present the hypothesized cell-assembly quite well in certain tasks.

This research is aiming at revealing the correlation between the neuronal discharge patterns with arm movement directions, and possibly further more, other information encoded in the discharge patterns such as movement speed, curvature, etc. Our preliminary results this far have shown promises of using SOFM as a computational tool to achieve the above objective. In particular due to the nonlinear nature of the network, the complex correlation between discharge rates and movement information are not confined by some linear relations as the population vector algorithm, the OLE method, or others. Furthermore, the SOFM does not require preferred directions of individual cells as prerequisites.

References

[1] Georgopoulos, A. P., J. F. Kalaska, R. Caminiti, and J. T. Massey (1982). "On the relations between the direction of two-dimensional arm movements and cell discharge in primate motor cortex". *J Neurosci* 2: 1527-1537.

[2] Georgopoulos, A. P., J. F. Kalaska, M. D. Crutcher, R. Caminiti, and J. T. Massey (1984). "The representation of movement direction in the motor cortex: single cell and population studies". In: *Dynamic Aspects of Neocortical Function.* (ed. GM Edelman, WE Goll, WM Cowan) New York; Neurosciences Research Foundation, Inc. pp. 501-524.

[3] Georgopoulos, A. P., J. T. Massey (1988). "Cognitive spatial-motor processes 2. Information transmitted by the direction of two-dimensional arm movement and by neuronal populations in primate motor cortex and area 5". *Exp. Brain Res.* 69: 315-326.

[4] Schwartz, A. B., and A. P. Georgopoulos (1987). "Relations between the amplitude of two-dimensional arm movements and single cell discharge in primate motor cortex".. *Soc Neurosci Abstr* 13: 244.

[5] Schwartz, A. B., R. E. Kettner, and A. B. Georgopoulos (1987). "Primate motor cortex and free arm movements to visual targets in three-dimensional space. 1. Relations between singly cell discharge and direction of movement". *J Neurosci.* 8(8): 2913-2927.

[6] Georgopoulos, A. P., R. E. Kettner, and A. B. Schwartz (1988). "Primate motor cortex and free arm movements to visual targets in three-dimensional space. 2. Coding of the direction of movement by a neuronal population". *J Neurosci.* 8:2928-2937.

[7] Schwartz, A. B. (1993). "Motor cortical activity during drawing movement: population representation during sinusoid tracing". *J Neurophysiol.* 70: 28-36.

[8] Smyrnis, N., M. Taira, J. Ashe, and A. P. Georgopoulos (1992). "Motor cortical activity in a memorized delay task". *Exp. Brain Res* 92: 139-151.

[9] Georgopoulos, A. P., A. B. Schwartz, and R. E. Kettner (1986). "Neuronal population coding of movement direction". *Science* 233: 1357-1460.

[10] Abeles, M. (1991). *Corticonics*, Cambridge University Press.

[11] Kohonen, T. (1988). "The "neural" phonetic typewriter," *Computer,* 21(3):11-22.

[12] Kohonen, T. (1988). *Self-organization and associative memory,* Springer Series In Information Sciences, Springer-Verlag, Berlin, Heidelberg, New York, 2nd edition.

[13] Kohonen, T. (1990). "The self-organizing map," *Proceedings of the IEEE,* Vol. 78, No. 9, pp. 1464-1480.

[14] Kohonen, T. (1991). "Self-organizing maps: optimization approaches," In T. Kohonen, K. Makisara, O. Simula, J. Kangas, editors, *Artificial Neural Networks,* North-Holland, June 1991, pp. I-981-990.

[15] Kohonen, T. (1995). *Self-organizing map,* Springer, Berlin Heidelberg, New York.

[16] Lin, S., J. Si, and A. B. Schwartz (1997). "Self-organization of firing activities in monkey's motor cortex: trajectory computation from spike signals," *Neural computation.* March, 1997.

[17] Nasrabadi, N. M., and Y. Feng (1988). "Vector quantization of images based upon the Kohonen self-organizing feature maps," *IEEE International conference on Neural Networks,* 1101-1108, San Diego.

[18] Obermayer, K. H., H Ritter, and K. Schulen (1990). "Large-scale simulations of self-organizing neural networks on parallel computers: application to biological modeling," *Parallel computing,* 14:381-404.

[19] Ritter, H and K. Schulten (1986). "Topology conserving mappings for learning motor tasks," *AIP Conference Proceedings,* Snowbird, Utah, 151:376-380.

[20] Schwartz, A.B. (1994). "Direct cortical representation of drawing," *Science,* 265: 540-542.

[21] Yair, E; K, G. Zeger (1992). "Competitive learning and soft competition for vector quantizer design," *IEEE Trans. on signal processing,* 40(2): 294-309.

[22] Lukashin, AV, and Georgopoulos, AP. (1994) "A neural network for coding of trajectories by time series of neuronal population vectors". *Neural Computation*, 6: 19-28.

[23] Salinas, E., and Abbott, LF. (1994) "Vector reconstruction from firing rate". *Journal of Computational Neuroscience*, 1: 89-108.

[24] Hebb, D. O. (1949). *The Organization of Behavior*, Wiley, New York.

[25] Vaadia, E., E. Ahissa, H. Bergman, and Y. Lavner (1991). "Correlated activity of neurons: a neural code for higher brain function. In *Neural Coopertivity.* Kruger, J., eds. Sprigner-Verlag, 249-279.

[26] Bizzi, E., N. Accornero, W. Chapple, N. Hogan (1984). "Posture control and trajectory formation during arm movement", *J. Neurosci.* 4: 2738-2744.

[27] Soechting, J. F. and F. Lacquaniti (1981). "Invariant characteristics of a pointing movement in man", *J. Neurosci.* 1: 710-720.

[28] Lacquaniti, F., J. F. Soechting, C. A. Terzuolo (1982). "Some factors pertinent to the organization and control of arm movements", *Brain Res.* 252:394-397.

[7] Schwartz, A. B. (1993). "Motor cortical activity during drawing movement: population representation during sinusoid tracing". *J Neurophysiol.* 70: 28-36.

[8] Smyrnis, N., M. Taira, J. Ashe, and A. P. Georgopoulos (1992). "Motor cortical activity in a memorized delay task". *Exp. Brain Res* 92: 139-151.

[9] Georgopoulos, A. P., A. B. Schwartz, and R. E. Kettner (1986). "Neuronal population coding of movement direction". *Science* 233: 1357-1460.

[10] Abeles, M. (1991). *Corticonics*, Cambridge University Press.

[11] Kohonen, T. (1988). "The "neural" phonetic typewriter," *Computer,* 21(3):11-22.

[12] Kohonen, T. (1988). *Self-organization and associative memory,* Springer Series In Information Sciences, Springer-Verlag, Berlin, Heidelberg, New York, 2nd edition.

[13] Kohonen, T. (1990). "The self-organizing map," *Proceedings of the IEEE,* Vol. 78, No. 9, pp. 1464-1480.

[14] Kohonen, T. (1991). "Self-organizing maps: optimization approaches," In T. Kohonen, K. Makisara, O. Simula, J. Kangas, editors, *Artificial Neural Networks,* North-Holland, June 1991, pp. I-981-990.

[15] Kohonen, T. (1995). *Self-organizing map,* Springer, Berlin Heidelberg, New York.

[16] Lin, S., J. Si, and A. B. Schwartz (1997). "Self-organization of firing activities in monkey's motor cortex: trajectory computation from spike signals," *Neural computation.* March, 1997.

[17] Nasrabadi, N. M., and Y. Feng (1988). "Vector quantization of images based upon the Kohonen self-organizing feature maps," *IEEE International conference on Neural Networks,* 1101-1108, San Diego.

[18] Obermayer, K. H., H Ritter, and K. Schulen (1990). "Large-scale simulations of self-organizing neural networks on parallel computers: application to biological modeling," *Parallel computing,* 14:381-404.

[19] Ritter, H and K. Schulten (1986). "Topology conserving mappings for learning motor tasks," *AIP Conference Proceedings,* Snowbird, Utah, 151:376-380.

[20] Schwartz, A.B. (1994). "Direct cortical representation of drawing," *Science,* 265: 540-542.

[21] Yair, E; K, G. Zeger (1992). "Competitive learning and soft competition for vector quantizer design," *IEEE Trans. on signal processing,* 40(2): 294-309.

[22] Lukashin, AV, and Georgopoulos, AP. (1994) "A neural network for coding of trajectories by time series of neuronal population vectors". *Neural Computation*, 6: 19-28.

[23] Salinas, E., and Abbott, LF. (1994) "Vector reconstruction from firing rate". *Journal of Computational Neuroscience*, 1: 89-108.

[24] Hebb, D. O. (1949). *The Organization of Behavior*, Wiley, New York.

[25] Vaadia, E., E. Ahissa, H. Bergman, and Y. Lavner (1991). "Correlated activity of neurons: a neural code for higher brain function. In *Neural Coopertivity.* Kruger, J., eds. Sprigner-Verlag, 249-279.

[26] Bizzi, E., N. Accornero, W. Chapple, N. Hogan (1984). "Posture control and trajectory formation during arm movement", *J. Neurosci.* 4: 2738-2744.

[27] Soechting, J. F. and F. Lacquaniti (1981). "Invariant characteristics of a pointing movement in man", *J. Neurosci.* 1: 710-720.

[28] Lacquaniti, F., J. F. Soechting, C. A. Terzuolo (1982). "Some factors pertinent to the organization and control of arm movements", *Brain Res.* 252:394-397.

[29] Soechting, J.F., F. Lacquaniti, C.A. Terzuolo (1986). "Coordination of arm movement in three-dimensional space. Sensorimotor mapping during drawing movement", *Neuroscience*. 17: 295-311.

[30] Soechting, J.F., C.A. Terzuolo (1987). "Organization of arm movements. Motion is segmented", *Neuroscience*. 23: 39-51.

[31] Soechting, J.F., C.A. Terzuolo (1987). "Organization of arm movements in three-dimensional space. Wrist motion is piece-wise planar", *Neuroscience*. 23: 53-61.

[32] Viviani, P., and N. Stucchi (1989). "The effect of movement velocity on form perception: geometric illusions in dynamic displays", *Percept. Psychophys*. 46: 266-274.

[33] Viviani, P., and C. Terzuolo (1982). "Trajectory determines movement dynamics", *Neuroscience*, 7: 431-437.

[34] Lacquaniti, F., C. Terzuolo, and P. Viviani (1983). "The law relating kinematic and figural aspects of drawing movements", *Acta Psychol*. 54: 115-130.

[35] Georgopoulos, A.P., R. Caminiti, J.F. Kalaska, and J.T. Massey (1983). "Spatial coding of movement: a hypothesis concerning the coding of movement direction by motor cortical populations". *Exp. Brain Res.*, Suppl. 7, pp. 327-336.

[36] Bizzi, E., N. Accornero, W. Chapple, and N. Hogan (1982). "Arm trajectory formation in monkeys". *Exp. Brain Res.*, 46: 139-143.

[37] Schwartz, A. B., and D. Moran (1997). "Motor cortical activity during drawing movements: population representation during lemnifcate drawing". *J Neurophysiol.* (in review).